

# Determination of cure mechanism inside die for a part manufacturing during large-scale pultrusion.

MUKHERJI, A., TARAPORE, N. and NJUGUNA, J.

2022

*This is the peer reviewed version of the following article: MUKHERJI, A., TARAPORE, N. and NJUGUNA, J. 2022. Determination of cure mechanism inside die for a part manufacturing during large-scale pultrusion. Journal of applied polymer science [online], 139(17), article 52035, which has been published in final form at <https://doi.org/10.1002/app.52035>. This article may be used for non-commercial purposes in accordance with Wiley Terms and Conditions for Use of Self-Archived Versions. This article may not be enhanced, enriched or otherwise transformed into a derivative work, without express permission from Wiley or by statutory rights under applicable legislation. Copyright notices must not be removed, obscured or modified. The article must be linked to Wiley's version of record on Wiley Online Library and any embedding, framing or otherwise making available the article or pages thereof by third parties from platforms, services and websites other than Wiley Online Library must be prohibited.*

# **Determination of Curing Mechanism Inside Die for a Part Manufacturing During Large Scale Pultrusion**

Arindam Mukherji<sup>1</sup>, Nozer Tarapore<sup>1</sup> and James Njuguna<sup>2\*</sup>

<sup>1</sup>SP Advance Engineering Materials Pvt Ltd, SP Centre, 41/44, Minoo Desai Marg, Colaba, Mumbai. 400 005, India, Email: arindam.mukherji@shapoorji.com

<sup>2</sup>Centre for Advanced Engineering Materials, School of Engineering, Robert Gordon University, Garthdee Road, Aberdeen, AB10 7GJ United Kingdom

\*Author to whom correspondence should be addressed; E-Mail: j.njuguna@rgu.ac.uk, Tel.: +44 (0) 122 426 2304

## **Abstract**

The cure kinetics of resin, heat capacity and thermal conductivity of reinforcing materials of uncured mass dictates the ultimate curing of reinforced thermosets manufactured component. In this study, degree of conversion from heat capacity by ‘Lumry and Eyring Model’ and order of reaction by multi- regression technique using ‘Borchardt and Daniels Model’ are calculated in finding cure kinetics ( $\gamma$ ) of the resin. Experimental results from differential scanning calorimetry (DSC), thermogravimetry (TGA) and rheological measurements were used to determine thermal conductivity, heat capacity and rheological parameters of the resin through several model fitting. The calculated thermal conductivity of uncured composite from ration of (length vs contact area) and thermal resistivity extracted from TGA data was fitted into specific mathematical model which predicts the thermal behaviour of heated prepreg during pultrusion operation. These parameters used in a separate mathematical partial differential equation-based model equation to predict the change in temperature and resin conversion along axial distance and radial thickness. The influence of operating conditions, such as rate of heating (Early and late Heating) and fibre volume fraction while curing inside die were calculated and validated with experimental results. This study evaluates the extent of heat transfer and degree of conversion inside pultrusion die during scale up steady state process. It is observed that paradigm of influencing parameters like pulling speed, die radial thickness and heater engagement (Early and late heating) on heat flow from die wall to core (i.e., thickness of the part being pulled) follows the data captured experimentally.

## 1. Introduction

Nowadays aerospace, military, automotive and construction find products from fibre-reinforced composites (FRP). Compared to many techniques like compression, filament winding, vacuum infusion, and transfer moulding for FRP manufacturing, pultrusion is widely preferred due to Low process cost consistent and continuous technique. Open bath conventional Pultrusion is the easiest way of impregnating resin to reinforcing materials. Critical factors influence pultrusion manufacturing operation are choice of line speed of pulling, pot life of the resin, die temperature for the profile, die geometry, die-heater arrangement to axial distance, reinforcement configuration and its impregnation with formulated resin. Complexity of process of impregnation of resin and its subsequent curing during pulling operation through heated die can be simplified by a Comprehensive Modelling. In studies of close pultrusion, pressure rise in the die inlet contributes to a major extent in enhancing wet-out and suppressing void formation in the manufactured composite wherein the resin injection pressure of closed pultrusion, pressure squeezed fibres together to an extent of essentially impenetrable of liquid resin [1-2]. Studies available mould filling process and impregnation of the reactive polymer of resin transfer moulding (RMT) by non-isothermal 3-D computer simulation model [3]. Effect of fibre mat presence (in the mould cavity) on the inlet pressure, pressure build-up in die, flow patterns and composite void content and temperature distribution can be modelled by taking lumped and un-lumped temperature during operation [4,5]. Although vast research works on closed injection die pultrusion are available but limited studies are found on open bath pultrusion. Finite elemental analyses by different methods can be used in predicted profiles temperature and degree of cure in a pultruded glass-fibre composite [6,7].

Many instrumental analyses like DCS, Dynamic Mechanical Analyser (DMA) Viscosity - rheometers at dynamic or Isothermal Moods were carried to capture the functional data. [8,9] TGA, DSC, Hot Disk, and DMA are very effective tool in validating temperature-dependent theoretical models for thermo-physical and mechanical properties polymers [10]. DSC can be used in measuring thermal conductivity and cure kinetics of solid materials thermosetting polymers [11,12]. Cure kinetic and rheological parameters of resin measured by DSC and Viscometer instruments may be used to comprehend influence of operating conditions, like line speed and heating rate on curing in the pultrusion die used [13,14]. Heat flow in die gets affected by line speed, material configuration, cure kinetics of formulated resin and die thickness. Numerical, theoretical, and empirical models on efficacy of heat transfer and thermal

effects of cure reaction by proposing kinetic model for heat transfer by finite element analysis, quadratic algorithmic programming and a particle swarm heuristic, promising heat and mass transfer equation resin cure reaction using conservation of mass, momentum, and energy during pultrusion, were used, and established for unsaturated polyester of in optimising pultrusion operation [15,17-20]. Integral method for heat transfer can be used in finding in changes in degree of cure and temperature distribution in materials due to start up and change in pultrusion operation condition during pulling [16].

Apparently thermal conductivity and rate of curing are most fundamental properties to evaluate the construction of materials but prediction of resin curing inside the die as function line speed is core important in designing the parts. Hence resin conversion and temperature distributions must be considered to model heat transfer along the axial length of pultrusion die during process as explained by [7].

2D and 3D heat transfer models were proposed by several researchers based on the theory of energy balance. The thermochemical problem of pultrusion is controlled by three governing Equation, i) for the tool, ii) for moving uncured beds of composites and iii) transport equation for resin.

For 3-D modelling, considering heat flow in three directions:

$$\rho * Cp * \left(\frac{\delta T}{\delta t}\right) - \left[\frac{\delta}{\delta x} \left(K_x * \frac{\delta T}{\delta x}\right) + \frac{\delta}{\delta y} \left(K_y * \frac{\delta T}{\delta y}\right) + \frac{\delta}{\delta z} \left(K_z * \frac{\delta T}{\delta z}\right)\right] = 0 \quad (1)$$

$$\rho * Cp * \left(\frac{\delta T}{\delta t} + U_x * \frac{\delta T}{\delta x}\right) - \left[\frac{\delta}{\delta x} \left(K_x * \frac{\delta T}{\delta x}\right) + \frac{\delta}{\delta y} \left(K_y * \frac{\delta T}{\delta y}\right) + \frac{\delta}{\delta z} \left(K_z * \frac{\delta T}{\delta z}\right)\right] - q = 0 \quad (2)$$

$$\frac{\delta \alpha}{\delta t} + U_x * \frac{\delta \alpha}{\delta z} = \gamma, \quad (3)$$

where  $q$ , is internal heat generated =  $\gamma * V_r * \rho_r * H_r$ , where  $\rho$ , density;  $Cp$ , specific heat ;  $V_r$ , is volume fraction of resin,  $H_r$  is total heat of reaction,  $K$  is thermal conductivity composite;  $U_x$  is pull-speed; and  $x$  is the pull direction;  $t$  is time and Subscript  $c$  denotes composites.

For 2-Dimensional, flow of heat is considered in  $x$  and  $z$  (radial) direction.

$$\rho * Cp * \left(\frac{\delta T}{\delta t}\right) + \rho_r * Cp_r * \left(V * \frac{\delta T}{\delta x}\right) = K_c [\Delta * \Delta T] + \gamma * V_r * \rho_r * H_r \quad (4)$$

Transit Heat      Convection Heat      Conduction      Internal Heat

(Considering  $K_c$  thermal conductivity in three axes as  $K_x$ ,  $K_y$  and  $K_z$ )

Where  $\Delta * \Delta T = \left(\frac{\delta}{\delta x} * K_x * \frac{\delta T}{\delta x}\right) + \left(\frac{\delta}{\delta y} * K_y * \frac{\delta T}{\delta y}\right) + \left(\frac{\delta}{\delta z} * K_z * \frac{\delta T}{\delta z}\right)$ .

Considering cure condition, where there is no flow of resin and velocity of resin is zero, the expression is,

$$\rho * C_p * \left(\frac{\delta T}{\delta t}\right) = K_z \left[\left(\frac{\delta}{\delta z} * \frac{\delta T}{\delta z}\right)\right] + \gamma * V_r * \rho_r * H_r \quad (5)$$

Again, the resin conversion is predictive to molecular or effective diffusivity and mass dispersity results from microscopic flow.

$\varphi * \left(\frac{\delta \alpha}{\delta t}\right) + (V * \Delta \alpha) = De * \varphi [\Delta * \Delta \alpha] + \gamma$ , where molecular diffusivity 'De' is very small and can be considered as zero. Hence expression would be as same as

$$\frac{\delta \alpha}{\delta t} + \left(\frac{v}{\varphi}\right) * \frac{\delta \alpha}{\delta x} = De * [\Delta * \Delta \alpha] + \gamma, \quad (6)$$

where v is the velocity of resin mostly in longitudinal direction and bare minimum in z and y direction, As condition prevails in gelling, v is consider zero, hence the equation turns to

$$\frac{\delta \alpha}{\delta t} = De * [\Delta * \Delta \alpha] + \gamma, \quad (7)$$

and for 2-D modeling , the expresion will be as

$$\frac{\delta \alpha}{\delta t} = De * \frac{\delta}{\delta z} \left(\frac{\delta \alpha}{\delta z}\right) + \gamma, \quad (8)$$

Determination of cure-kinetics at the backend evaluates the degree of conversion and rate of conversion which gets perturbed by interaction of reinforcing materials and other ingredient during pultrusion, interference due to heat transfer or heat flow through die wall during external heating and internal exothermic reaction heat. Eventually all parameters are potentially influenced by the speed of pulling. On the other hand, curing of polyester is very complex involves multiple competing reactions which gets initiated by decomposition of initiators and crosslinking to have 3-D network formation by styrene monomers. Hence, the knowledge of the cure mechanisms during pultrusion process is becoming increasingly important for engineering application and developments. The complication of curing of resin in Pultrusion can only be simplified by comprehensive mathematical modelling.

In this study, we evaluated the extent of heat transfer using 2-D heat transfer Model (Eqs.4-8) derived from 3-D heat transfer Model (Eqs.1-3). Wherein dimensionless time, temperature, and conversion (Eqs.57-59) were used to simulate conversion and temperature with Die axial distance and its Thickness, speed of pulling and rate of heating during scale up steady state process. Predicted Thermal conductivity (Eqs.43-56) of cured and uncured composites from

ration of (length vs contact area) and thermal resistivity through single scan differential scanning calorimeter (DSC) may not consider the influence of compaction in die during gelation and the heat capacity of individual materials. TGA estimates volume fraction to avoid situational concoction due to air trapped during curing. The calculated thermal conductivity of uncured composite was fitted into specific mathematical model, predicts thermal behaviour of heated prepreg during pultrusion operation. Again, Pre-exponent Factor, degree of conversion from heat capacity by 'Lumry and Eyring Model' (Eqs.9-20) and order of reaction by multi-regression technique using 'Borchardt and Daniels Model'(Eqs.21-42) are calculated in finding cure kinetics ( $r_a$ ) of the resin. Calculated parameters like thermal conductivity, heat capacity and reaction kinetics from dependent models were fitted into Heat transfer model to simulate part behaviour inside open bath Pultrusion Heated discontinued die during pulling. Results found endorse processor to configure process parameter, material combination and heater engagement in getting steady pulling in operation with limited impute data.

## **2. Experiment**

### **2.1. Material**

A continuous random glass fibre mats with 450 and 300 g/m<sup>2</sup> (gsm) was provided by Skaps Industries India PVT Ltd. A glass roving of 4800 tex (tex: the mass in gram per one kilometre of a fibre roving) was provided by Owens Corning. A combination of continuous random glass mats and glass roving fibre package of 600 gsm was used. From SIGMA –ALDRICH Precipitated calcium carbonate (CaCO<sub>3</sub>) powder from Gulshan Polyols Limited, was employed as the conventional micron-filler. Orth phthalic acid based unsaturated polyester resin (MECHSTER™ 9000P) tailored for the pultrusion process from Mechamco was used in this study.

### **2.2. Pultrusion Line and Experiment set up**

Figure 1(a) shows a schematic of pultrusion line used in this work. The line consists of creel stands for roving and racks for felts, veil fabrics and unwinding continuous filament- mat (CFM), a resin tank, a pre-forming assembly composed of perforated steel plates and other guid rollers, a heated die, die with heating elements along its length, a pulling unit and a flying cut-off saw. Temperature profiles along the die, pulling force, pulling speed, and pressure inside die are measured and recorded in data form. Hydraulic oil pressure exerted during pulling is

monitored through PLC controlled pulling unit. This pultrusion pulling unit can either be used for open bath or closed die Pultrusion. In our regime open bath pultrusion with 300 mm discontinued tapping section used as shown in Figure 1(b) with 100 mm of die discontinuity Gap maintained by placing heat insulative asbestos sheets.

Wetting of reinforcing fibres are very crucial for any composite part without dry patches. Figure 1(a), an open bath impregnation technique, used to wet fibres by pulling fibres through resin tank. To ensure all fibres are sunk under resin, system does not allow resin level to go down below specified limit. Higher pulling speed and entangled fibres are avoided for better wettability. Impregnated fibres are guided through guide rollers and plate and finally through preforming assemble to have specified part cross section prior to entire into die. Plane textiles like polyester veils may also be pulled through the resin bath or wetted out by excess of resin carried by roving on entering the die. Excess resin and trapped air are squeezed out by discontinued compaction tapper section, so that pultruded parts of low void can be produced. Curing to solidification of profile is made by passing the squeezed material through heated die.

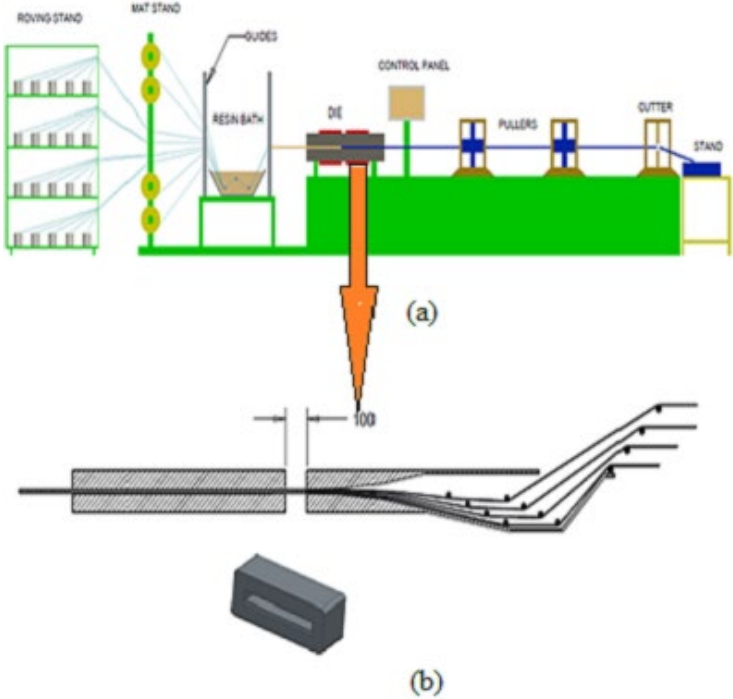


Figure 1(a): Schematic diagram of open bath pultrusion

Figure 1(b): The schematic of Compaction Zone in Conventional Pultrusion Die with 100 mm discontinuity gap

The die temperature management is crucial to produce good quality components, hence a gradual increase in resin temperature is achieved by placing more heating plates, turn out zones with different set temperatures along the length of the die.

As the mats travelled through the die, temperature was recorded by thermal sensor placed in between the layers at time when mat enters die. The fibre-package consisted of 10 layers of Bidirectional mats with 600 g/m<sup>2</sup> and 60 roving with 4800 tex. The thickness of the produced composites was 8 mm. Experiment were carried out to measure the pulling force change during the start-up stage of high-pressure tapper die, Figure 1(b).

### **2.3. Characterisation**

Thermogravimetry (TG) was performed on a TAG -50, Shimadzu instrument, using hermetic pans and sample weights lower than 6 mg. Both isothermal and dynamic scans were run at temperatures typically around at 380°C or heating rates between 2.5 °C/min respectively up to 380 °C. Herein for solid product characterisation, preregs of reinforcing fibres impregnated in polyester resin were used. Preregs used contained similar proportion of resin and reinforcing fibres as in product characterised by TG. Decomposition temperature and reduction of wt.% using tetra methyle ammonium hydroxide allowed evaluation of composition of products.

The differential scanning calorimetry (DSC) was performed on a TA-60 Plus Shimadzu instrument, using hermetic pans and sample weights lower than 10 mg. The used materials in the experiments are formulated in resin paste and different low conversion as mentioned in Table 1. Both isothermal and dynamic scans were run at temperatures typically around 60 °C to 80 °C or heating rates between 3 and 15 °C/min respectively. All curatives and additives are premixed separately before sampling. The sample preparation should be done swiftly to avoid loss volatiles like styrene results in loss of data during the first stages of the reaction. In our study rheological measurements were performed on a Brookfield Viscometer with hot water bath arrangement in similar approach of cure process epoxy prepreg analysed through thermal rheological parameters by [21] Sun (2002). The resin was poured in a beaker which attached to holder to maintain steady state. The time dependent increase in viscosity (Pa.s) during isothermal runs at temperatures typically between 60 °C and 80 °C was monitored with single spindle at a definite torque.

**Table 1. Materials and formulation used for the friction measurement**

<b>Ortho -Polyester resin</b>	Mechemco	100 phr
<b>Perkadox-C</b>	Ackzonoble	0.05 phr
<b>MEKP</b>	Aldrich Chemical	0.25–0.50 Phr
<b>BPO</b>	Veekay Chemicals	1.0 Phr
<b>TBPB</b>	Veekay Chemicals	1.2 Phr
<b>Calcium Carbonate -400</b>	GULSHAN Polyols Limited	30 pbw
<b>Release Oil</b>	Fine Organics	1 pbw

### 3. Results and Discussions

#### 3.1. Thermal properties

Figure 2 shows the dynamic DSC of formulated resin at different rate of heating. The maximum peak shifts to higher temperatures with increasing heating rates. The relative area under the curves up to a given temperature is good measure of the total heat required for complete curing which supports in finding degree of conversion. From the figure 2, it is found that area under curve escalates with increasing rate of heating (2-20 °C/min), which manifests increase of total heat content. This phenomenon may be explained by diffusion theory of resin. Due to faster gelling, heat transfer experienced hindrance by higher viscous resin. It is reported that T-values and the thermal stability of polymers arising from the isothermal cure were generally higher than those for the corresponding dynamic cure [22]. A relation found between Glass-Transition Temperature and its conversion for epoxy by relating delay reaction [23, 22]. In the studies, all DSC curves an incline on the right side can be distinguished pointing at a delay of the reaction. This is due to gelation effect of fast heating rate which causes the reaction rate to become diffusion controlled.

Again, from DSC thermograms, it is observed the heat of reaction increases with increasing rate of heating and due to diffusion effect, curing takes more time. Even the 2<sup>nd</sup> stage of curing like high temperature curing or high temperature ( $T_g$  for thermoset composites) is well predicted from this graph. Arriving of 2<sup>nd</sup> peaks are more prominent as rate of heating increases. Hence complete curing takes at much higher temperature for higher rate of heating. The cure mechanism of GFRC during pultrusion process is explained in detail in the literature [24, 25]. As process of formulated resin inside the die during pultrusion gets cured by virtue of external

heat and exothermic heat of reaction. Hence to predict the thermal conductivity, the fibre volume fraction, resin volume fraction and volatile gas fraction which evolves during real time operation were determined from uncured composite samples taken from production master batch of pultruded products. The conductivity was divided into three phases. Phase one is composed of styrene gases evolved from uncured resin and other volatiles like moisture of fibres perceived as undecomposed phase, phase two composed of only

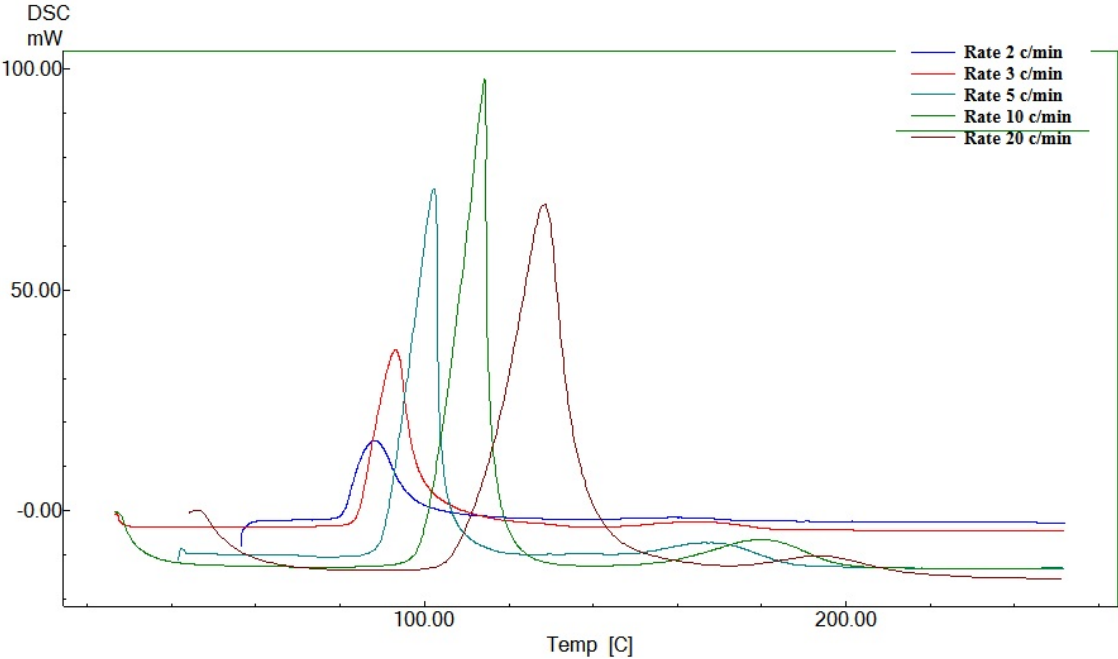
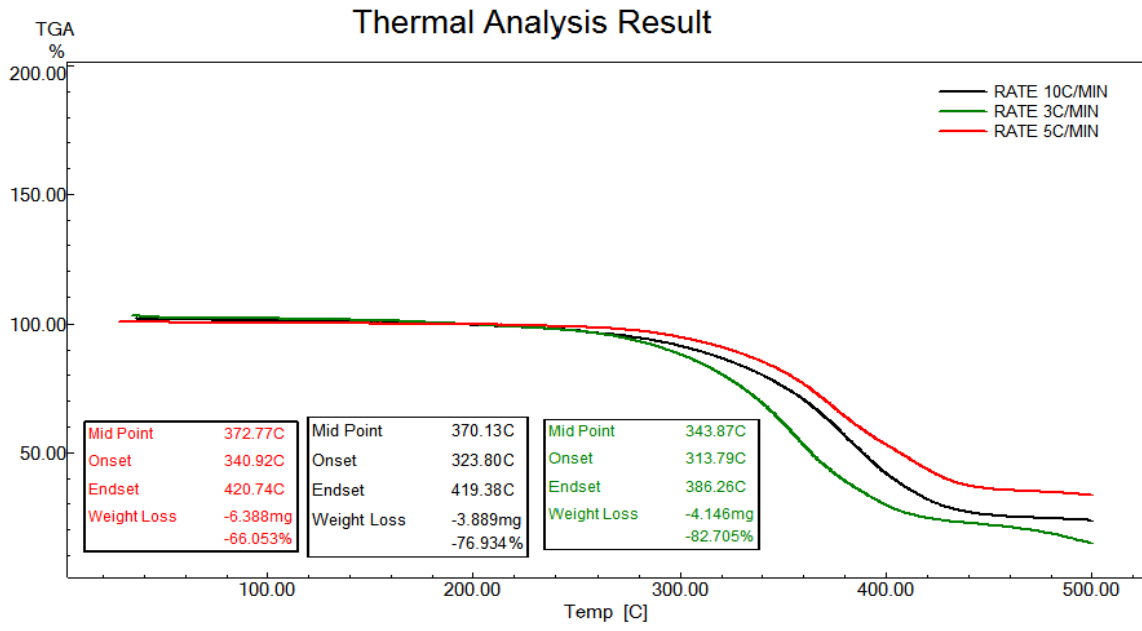
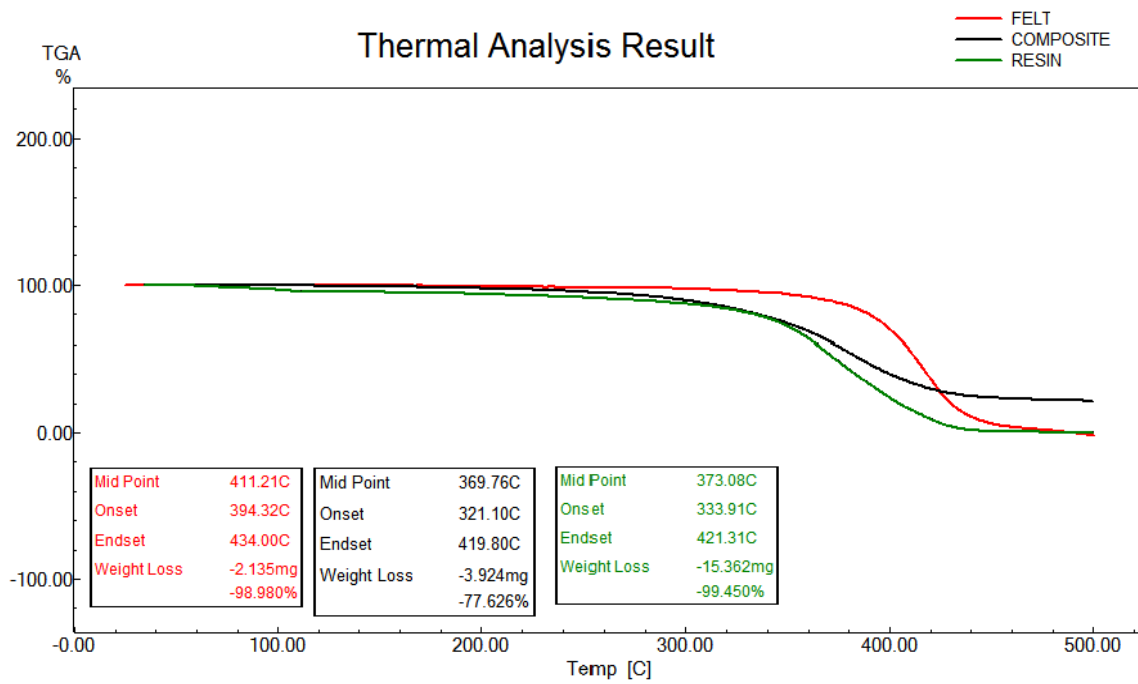


Figure 2: Dynamic DSC of Formulated polyester resin

decomposed material to comprehend the onset and end set temperature of being decomposed and third phase is after decomposed remaining filler and decomposed resins chars. Figure 3(a) presents the TGA profiles for the formulated polyester resin at different temperature while Figure 3 (b) shows TGA runs of virgin resin, uncured prepreg and recycled polymer fibres at 3°C/min rate of heating. From these thermograms, it was found out that the decomposition of resin starts above 373 °C and ends at 386°C wherein recycled polymers fibres starts decomposing beyond 390 °C and ends at 420°C. The analogue of prepreg at different rate of heating implicates lower rate of heating, brings higher material loss with



(a)



(b)

Figure 3: TGA profiles. (a) TGA profiles for the formulated Polyester resin at different temperature, (b) TGA thermograms of red is recycled polymer fibres/felt, black is polyester (composite) prepreg with recycled polymers fibres as reinforced, green is pure polyester resin

lower onset and end set temperature range compared to higher rate of heating. Analogue as shown in Figure 3(A & B) wt.% loss due to decomposition and volatile loss, composition and material weight contribution to composite product can easily be calculated; wherein for thermal conductivity, model fitting with volume fraction calculated from weight loss of uncured prepreg and pertinent heat involve with known contact area of TGA pans to evaluate resistivity of heat, conductivity was calculated during process of curing, as stated below in the Eqs.43 - 55.

Furthermore, curing behaviour gets influenced by heat flow inside the matrix as similarly predicted through mathematical modelling. This sudden rise in curing eventually increases the viscosity of the resin, a phenomenon observed in iso-thermal rheology. After an initial stage of a small viscosity build up the viscosity suddenly increases sharply as shown on Figure 4, an iso-thermal rheology of formulated resin at different temperature. The sudden increase in viscosity is a clear indication of network formation in increase in molecular weight due to crosslinking turns the system into semisolid-like behaviour from pure liquid-like behaviour.

Gelation time is accurately determined from half-life and the time required to reach the maximum cure rate as elucidated by isothermal cure kinetics of unsaturated polyester resin [26]. A simpler way can be to take the time when the viscosity reaches 10,000 PaS. As seen in Figure 2, the gelation process is faster and more abruptly at higher temperatures. The reaction more complicated and the diffusion phenomena is initiated by temperatures rise. If it is compared with highest peak in the dynamic DSC, it evident that rise in temperature is not complete of curing or complete of conversion but it indicates the starting of networking and eventually viscosity increases fast and conversion rates get reduced due to restriction of chain interaction. After gelation, the curing continues although the process is much slower because of the reactive groups are restricted in their movement. This limited diffusion effect also causes seldom failure to reach the complete conversion. Dynamic rheometric and temperature modulated DSC for slowing down molecular mobility during diffusion control is associated with the processes of gelation is demonstrated by Sbirrazzuoli, et al. [27].

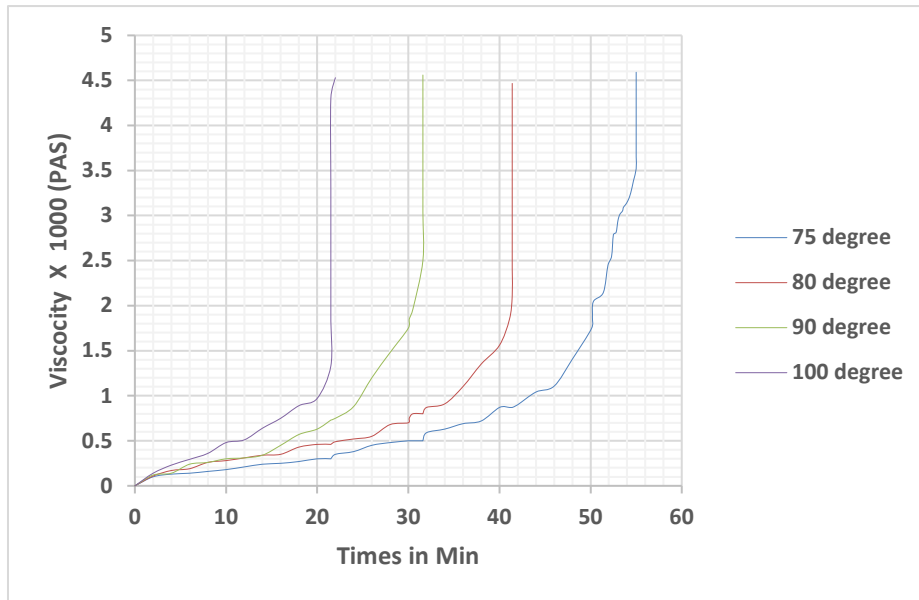


Figure 4: Change in viscosity of formulated resin with time sweep at different set temperature .

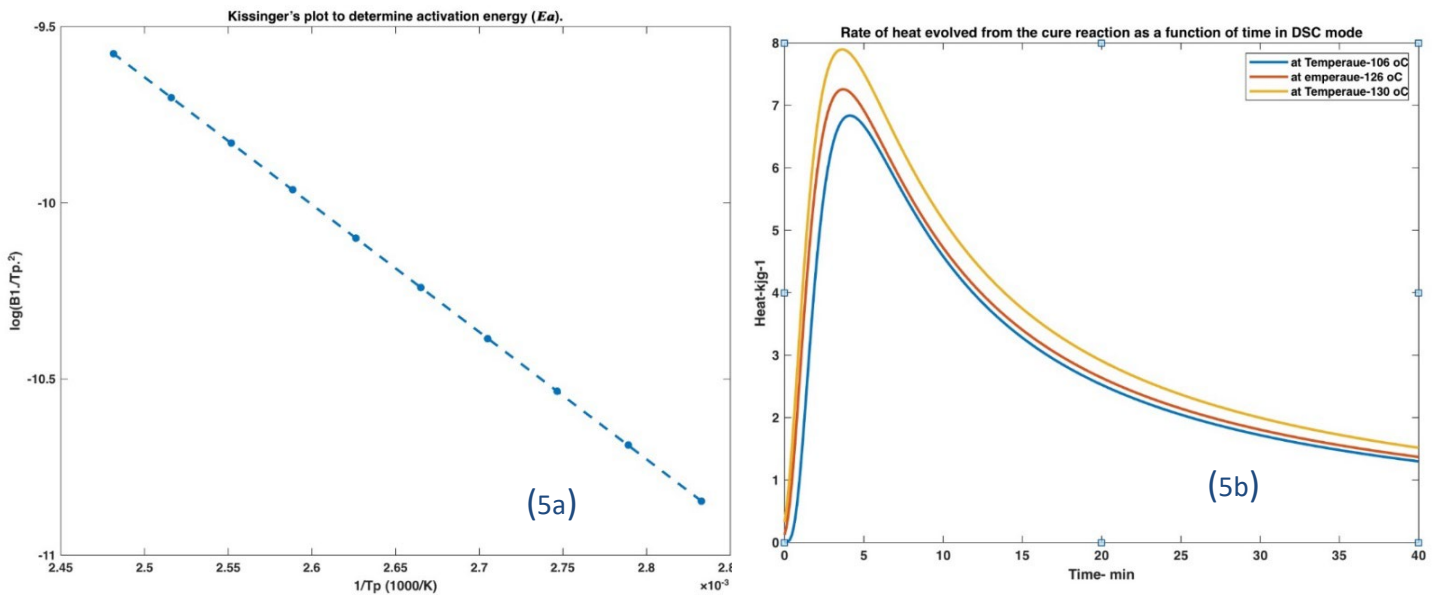


Figure (5a): Model fitting- Kissinger plot for activation energy of formulated resin.

(5b): Rate of heat evolution during cure reaction

### 3.2. Kissinger Method for Dynamic Scanning Curing Process for Activation Energy and Arrhenius Number (as Pre-exponent Factor).

From dynamic scanning with varying rate of heating, separate peak temperature is available for calculating Activation Energy ( $E_a$ ), Arrhenius number ( $Ar$ ), using Kissinger equation,

$$\ln(B/Tp^2) = \ln(Ar * R_g/E_a) - E_a/(R_g * Tp), \quad (9)$$

wherein R is universal gas constant and by plotting  $\ln(B/Tp^2) = \text{Vs } 1/Tp$ , value of  $E_a/R_g$  can be calculated from the slope and  $A_r$  (pre-exponent) can be calculated from the intercept on  $\ln(B/Tp^2)$  axis as plotted in Figure 5a. At constant temperature, rate heat evolves with time is higher for higher set temperature as depicted in figure (5b).

### 3.3. Degree of conversion from heat capacity using ‘Lumry and Eyring Model’

Temperature dependence of equilibrium constant ‘ $\dot{K}$ ’ can be expressed by

$$\dot{K} = X_u/X_n = \exp(-H_t/R_g * (1/T - 1/T_{1/2})) \quad (10)$$

where  $X_u, X_f$  and  $X_n$  is molar fraction at unfolded, final state and native state respectively, and  $T_{1/2}$  is temperature where  $\dot{K}=1$ , Similarly, rate constant ‘ $k$ ’ is expressed as

$$k = \exp(-E_a/R_g * (1/T - 1/T^*)) \quad (11)$$

$$\text{Since, } X_u + X_f + X_n = 1 \quad (12)$$

$$\text{and } X_u = (1 - X_f) * \dot{K}/(\dot{K} + 1) \quad (13)$$

$$dX_f/dT = 1/v * (\dot{K} * k/\dot{K} + 1)(1 - X_f) \quad (14)$$

on integrating

$$X_f = 1 - \exp(1/v * (\dot{K} * k/\dot{K} + 1) * (1 - X_f)) \quad (15)$$

$$X_u = \dot{K}/(\dot{K} + 1) * \exp(-1/v * \int_{T_0}^T [k * \dot{K}/(1 + \dot{K})] dT) \quad (16)$$

$$X_n = 1/(\dot{K} + 1) * \exp(-1/v * \int_{T_0}^T [k * \dot{K}/(1 + \dot{K})] dT) \quad (17)$$

$$Cp = H_t * (dX_n)/dT \quad (18)$$

$$\text{For any reversible model } Cp = (H_t^2/R_g * T^2) * \dot{K}/(\dot{K} + 1), \quad (19)$$

and for any irreversible model

$$Cp = (k/v + H_t/R_g * T^2) * \dot{K} * H_t/(\dot{K} + 1)^2 * \exp(-1/v * \int_{T_0}^T [k * \dot{K}/(1 + \dot{K})] dT) \quad (20)$$

A fair trajectory of increasing degree of conversion with time is observed from figure (6a) where from figure (6b) rate of conversion gets diminished after its peak when plotted with degree of conversion. It is worthy to mention, rate of change in degree found more on higher temperature.

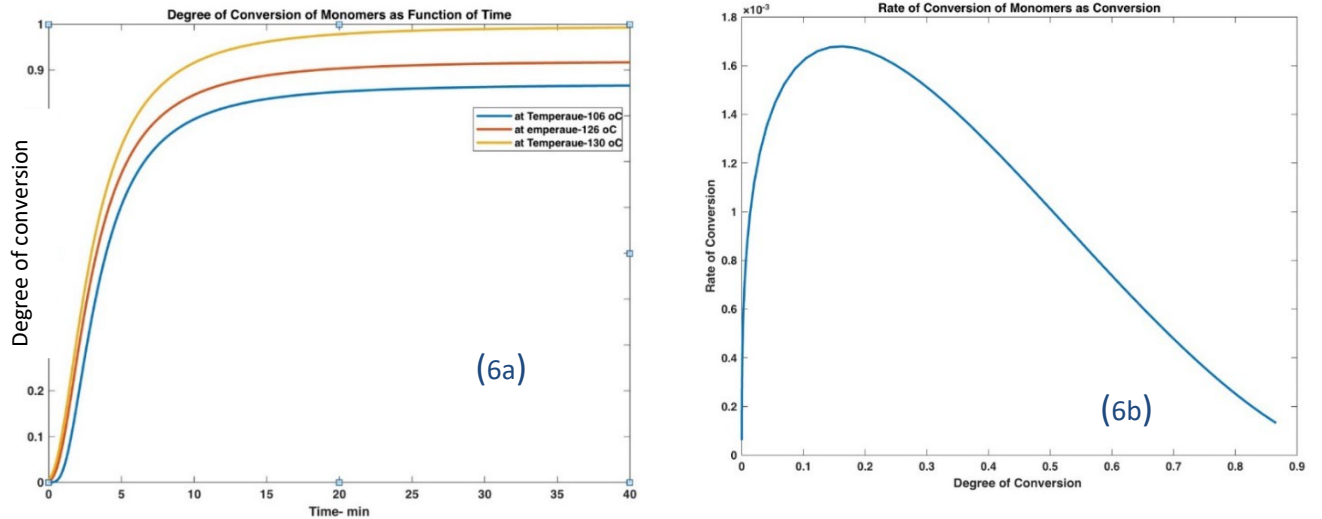


Figure (6a): Model fitting-degree of conversion with temperature sweep  
 (6b): Change in rate of conversion with degree of conversion at DSC mood

### 3.4. Borchardt and Daniels based model analyses order of cure reaction by multi-regression technique

In situ cure model parameter identification and sensing [28], and influence of ferro fluid in thermal-conductive of polymers [29], provides model analysis in finding order of reaction. From DSC , total degree of coversion can be clculated from available heat of reaction of partial area and total heat of rection as

$$\alpha = \left[ \frac{H_r(t)}{H_t} \right] \quad (21)$$

$$\frac{d\alpha}{dt} = \left( \frac{1}{H_t} \right) * \left( \frac{dH_r}{dt} \right) \quad (22)$$

change of degree of conversion with time can be calculated by integrating equeation (21). Similarly change of degree of conversion can be clculated from availabe change in temperaature during curing using DSC Isotherml scaning as shown in figure (7). Differential Scanning Calorimetry Technique can be used for measuring Reaction kinetics, Activation Energy and Preexponential Factor for thermoset resin [30].

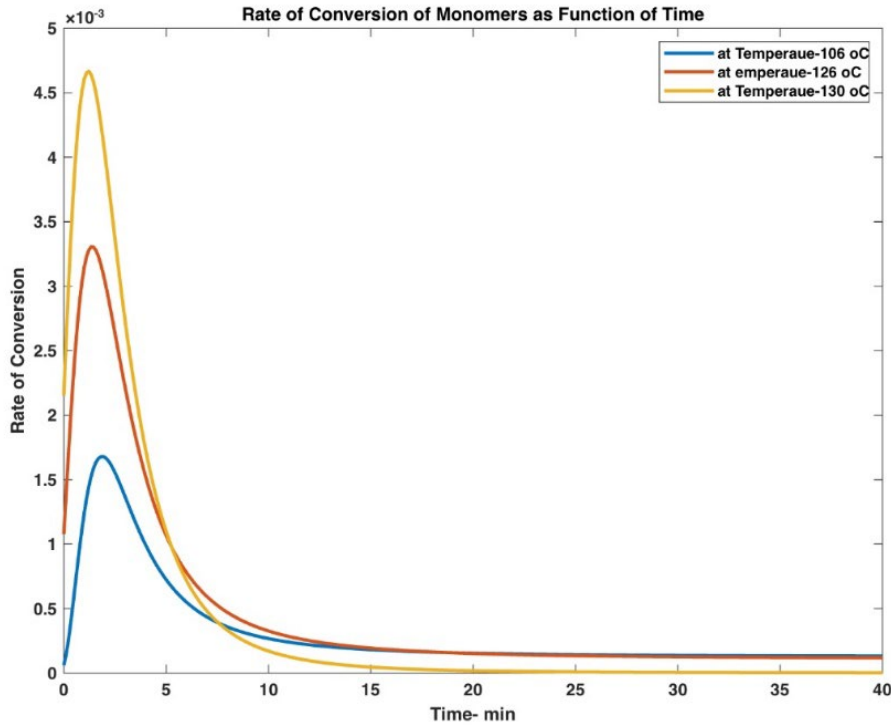


Figure 7: Model fitting -rate of conversion of monomers with time sweep at three different set temperature

$$\text{As } H_r = Cp * T, \text{ hence } \alpha_i = [(Cp * T_t) * T_i / H_t], \quad (23)$$

degree of conversion can also be calculated from change in viscosity with time experimentally. As viscosity is a combination of physical and chemical change ,

$$\eta = \Psi (T) * \zeta(\alpha) \quad (24)$$

Where  $T$  is for physical temperature and  $\alpha$  is degree of conversion change.

$$\Psi (T) = \eta_o, \quad (25)$$

In equation (25),  $\eta_o$  is the initial viscosity and

$$\zeta(\alpha) = 1/(1 - \alpha) \quad (26)$$

hence

$$\eta = \eta_o * 1/(1 - \alpha) \quad (27)$$

and again

$$\eta_o = A_\eta * \exp(E_n/R_g * T) \quad (28)$$

$$\eta = A_\eta * \exp(E_n/R_g * T) * 1/(1 - \alpha) \quad (29)$$

$$\alpha = 1 - A_\eta * \exp(E_n/R_g * T) / \eta \quad (30)$$

where in  $A_\eta$  initial viscosity at  $T=\infty$ , and  $E_n$  activation energy at viscous flow dependent on the resin/curative mix ratio.

From multiple linear regression, values for  $A_\eta$ , and  $E_n$  activation energy at viscous flow can be calculate from the expression as

$$\text{From Thermal model, } \frac{d\alpha}{dt} = K(T) * g(\alpha) \quad (31)$$

$$\frac{d\alpha}{dt} = K(T) * (1 - \alpha)^n \quad (32)$$

$$\int (1 - \alpha)^{-n} d\alpha = \int_0^t (K) dt \quad (33)$$

$$1/(1 - \alpha) = (1 + (n + 1) * \int_0^t (K) dt)^{1/(1-n)} \quad (34)$$

By taking log on both side,  $l$

$$n(\eta) = \ln(A_\eta) + E_n/R_g * T + (1 + (n + 1) * \int_0^t (K) dt)^{1/(1-n)} \quad (35)$$

$$\text{since } K = A_r * \exp(-E_a/R_g * T) \quad (36)$$

$$\ln(\eta) = \ln(A_\eta) + E_n/R_g * T + (1 + (n + 1) * \int_0^t (K) dt)^{1/(1-n)} \quad (37)$$

by multiple regression, and know value of  $E_a$ ,  $R$  and  $A_r$ , values of  $A_\eta$  and  $E_n$  can be calculated.

Substituting  $E_n$  and  $A_\eta$  on equaton, degree of conversion at specific time at Isotherml condition can be calculated.

$$\text{Now, } \frac{d\alpha}{dt} = K(T) * g(\alpha) \quad (38)$$

$$\frac{d\alpha}{dt} = \gamma = K(T) * \alpha^m * (1 - \alpha)^n \quad (39)$$

where in  $\gamma$ , is the rate of degree of converion,

$$K = A_r * \exp(-E_a/R_g * T), g(\alpha) = \alpha^m * (1 - \alpha)^n \quad (40)$$

considering ‘Prout-Tompkins Autocatalytic’ reaction model.

$$\gamma = A_r * \exp(-E_a/R_g * T) * \alpha^m * (1 - \alpha)^n \quad (41)$$

Taking log on bothside of equation (41), we have

$$\log(\gamma) = 1 * \log A_r + (-E_a/R_g * T) + m * \log a + n * \log(1 - a) \quad (42)$$

where  $\gamma$  is rate of curing,  $\alpha$  is the degree of curing or polymerisation,  $T$  is temperature,  $E_a$  is the activation energy for polymerisation,  $R$  is the universal gas constant and  $A_r$  is Arrhenius constant. From linear multiple regression method, order of reaction is calculated through a

MATLAB code formulation, multiple regression code,  $x_1 = \log a_1, x_2 = \log(1-a_1), x_3 = [1/T]; y = \log(\gamma)$ , we get all the coefficients of equation (41) with maximum error of 0.07, 0.08, 0.09. From different cure system, we get values like  $n=1.22, 0.69$  and  $0.72, m=0.91, 0.80$  and  $0.82, E_a=82.17, 74.3$  and  $74.42$

### 3.5. Thermal conductivity

Heat transfer over any particular area of contact can be evaluated by measuring the total thermal resistance. This thermal resistance comprises thermal resistance of the sample, thermal resistance due to contact between sample and Heat sink, and thermal contact resistance between sample and the heat source (furnace). From Fourier's law, heat transfer rate is proportionate to difference in temperature, contact area and inversely proportionate to depth of the sample. Similarly, thermal conductivity apparatus (Lees' disk) and DSC were used in finding of thermal conductivity of PTFE [31].

$$\text{Since } Q = \lambda * \delta T * A / L \quad (43)$$

where  $\lambda$  depicts average thermal conductivity,

$$\lambda = Q * L / \delta T * A \quad (44)$$

where term  $\delta T / Q$ , is a measure of thermal resistance ( $R$ ),

$R = R_1 + R_2 + R_3$ ,  $R_1$  &  $R_2$  are almost constant,

$$R_3 = \delta T / Q = L / (A * \lambda) \quad (45)$$

Now to minimise error due to voids, always take the volume of the individual substance can be estimated by TGA thermograms on thermal conductivity and ratio of length to area will be replaced by product of total phase length and volume fraction of individual material being exposed. During thermal degradation and subsequent transfer, Volume of Volatile loss, pure resin and other reinforcing material can easily be estimated by TGA instrument. Difference in temperature and Heat transfer during degradation measured from TGA will make thermal resistance ( $R$ ) available for plotting 2d linear Graph with ratio of Phase degradation Length for individual materials to Constant Area. Effect of thickness plays important role on polyester curing in vacuum infusion technique for making transparent glass laminated nanocomposite [32].

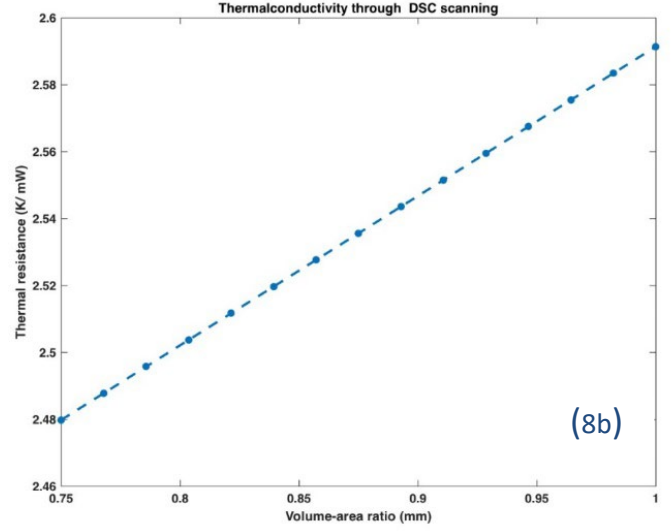
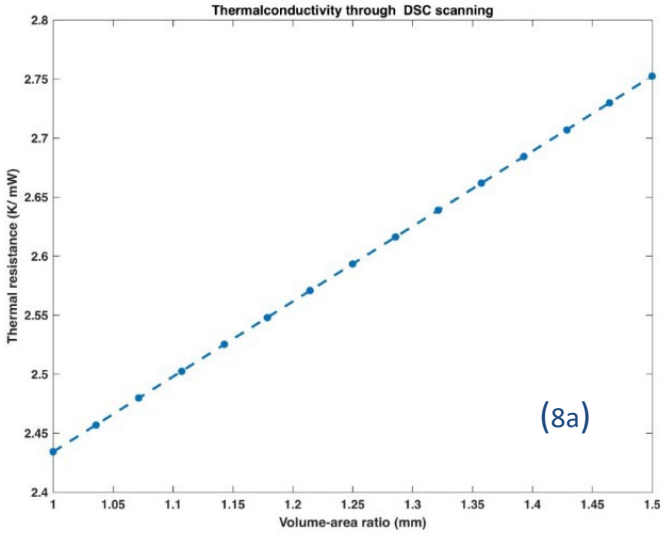


Figure (8a): Thermal resistance with volume-area ratio for resin  
 (8b): Thermal resistance with volume-area ratio for recycled felts, used as reinforcing materials.

Now the expression in eq.45 is replaced by

$$R3 = \delta T/Q = \delta X * \dot{V}/(A * \lambda) \quad (46)$$

$\delta X$  is total length of the phase being exposed. Now on plotting ratio of temperature range and difference of heat with ration of volume by contact area make slope available for  $1/\text{thermal conductivity}$  as shown in figure 8a and 8b.

One-dimensional model proposed [33,34], wherein thermal behaviour is analysed for FRP composites on exposed to fire. TGA thermograms of formulated resin, informs on the volatile loss and the peak temperature of degradation of the resin. Similarly, TGA thermogram of pure fibres present the peak temperature of decomposition. The TGA of cured sample allows to calculate the wt. % of fibres and polymer resin, i.e., the volume fraction is determined from theoretical density of each material in that,

$$\lambda_1 = [Q \delta X V_1]/[A. \delta T_1] \quad (47)$$

$$\lambda_2 = [Q \delta X V_2]/[A. \delta T_2] \text{ and} \quad (48)$$

$$\lambda_3 = [Q \delta X V_3]/[A. \delta T_3] \quad (49)$$

$$\lambda = [Q \delta X]/A. [\delta T_1 + \delta T_2 + \delta T_3] \quad (50)$$

Wherein considering total length  $\delta X$  and 1 as volume fraction

$$\text{and } \lambda = 1/[ (V_1/ \lambda_1) + (V_2/ \lambda_2) + (V_3/ \lambda_3)] \quad (51)$$

$$1/\lambda = [ (V_1/ \lambda_1) + (V_2/ \lambda_2) + (V_3/ \lambda_3)] \quad (52)$$

$$1/\lambda_{co} = V_a/\lambda_a + V_b/\lambda_b + V_c/\lambda_c \quad (53)$$

where  $V_a$  'low volatiles',  $V_b$  'Resin' and  $V_c$  remaining 'reinforcing fillers' volume fraction  
Similarly, thermal conductivity of un-decomposed composites can be equated as

$$1/\lambda_{uco} = V_a/\lambda_a + V_b/\lambda_b + V_c/\lambda_c, \quad (54)$$

for resin, we calculated the thermal conductivity as 0.4462 W/m·K and 0.6364 W/m·K for polymer reinforcing fibres. Thermal conductivity of low volatile material is taken as 0.03 W/m·K. Hence our composite thermal conductivity calculated as  $K_p = 0.4786$  W/m·K

$$\frac{\delta\alpha}{\delta t} = \frac{\delta^2\alpha}{\delta r^2} + \gamma \quad (55)$$

to simplify the heat transfer model, dimensionless variables were introduced where  $\theta$  is dimensionless temperature =  $T/T_0$ ,

$$T = \theta * T_0, \quad (56)$$

is the temperature in Kelvin and  $T_0$  is the initial temperature (298K)

$$\tau \text{ is dimensionless Time} = t * \lambda / [(P_c * Cp_c) * (D/2)^2] \quad (57)$$

$$\text{and therefore } t = \tau * [(P_c * Cp_c) * (D/2)^2] / \lambda \quad (58)$$

$\dot{x}$  is dimensionless radius of the die,  $\dot{x} = r/(D/2)$ ,

$$r = [\dot{x} * (D/2)] \quad (59)$$

$r$  is radial position and  $D$  is diameter of the die  $\dot{\alpha} = [\lambda/(P_c * Cp_c)]$  is the thermal diffusivity.

$$A = A_r * (D/2)^2 / \dot{\alpha}; \quad (60)$$

$$C = H_t / (Cp_c * T_0); \quad (61)$$

$$B = E_a / (R_g * T_0), \quad (62)$$

$$\dot{K} = \exp((-H_t/R_g) * (1/(T_0 * u(1)) - 1/328)), \quad (63)$$

$$Cp = H_t^2 * \dot{K} / (R_g * (T_0 * u(1))^2 * (\dot{K} + 1)^2), \quad (64)$$

$$\rho * Cp * \frac{\delta T}{\delta t} = \lambda \left( \left( \frac{\delta}{\delta r} \right) \left( \frac{\delta T}{\delta r} \right) + \frac{1}{r} * \left( \frac{\delta T}{\delta r} \right) \right) + \gamma * \rho * \Delta H \quad (65)$$

$$\frac{\rho * Cp * (\delta(\theta * T_0))}{\delta(\tau * [(P_c * Cp_c) * (D/2)^2] / \lambda)} = \frac{\lambda (\delta^2(\theta * T_0))}{\delta [\dot{x} * (D/2)]^2 + 1 / \gamma * (\delta(\theta * T_0) / \delta [\dot{x} * (D/2)])} + \gamma * \rho * \Delta H, \quad (66)$$

$$\frac{d\theta}{d\tau} = \left( \frac{d}{d\dot{x}} \frac{d\theta}{d\dot{x}} + \frac{1}{\dot{x}} * \left( \frac{d\theta}{d\dot{x}} \right) \right) + \frac{d\alpha}{d\tau} * C \quad (67)$$

$$\frac{\delta\alpha}{\delta t} = \left( \frac{\delta}{\delta r} \right) \left( \frac{\delta\alpha}{\delta r} \right) + \gamma, \quad (68)$$

$$\frac{\delta\alpha}{\delta(\tau * [(Pc * Cp_c) * (D/2)^2] / Kp)} = \left( \frac{\delta}{\delta r} \left( \frac{\delta\alpha}{\delta r} \right) \right) + \gamma \quad (69)$$

$$\text{Since } \gamma = A_r * \exp(-E_a/R_g * T) * \alpha^m * (1 - \alpha)^n \quad (70)$$

$$\frac{\delta\alpha}{\delta(\tau * [(Pc * Cp_c) * (D/2)^2] / Kp)} = \left( \frac{\delta}{\delta[\dot{x} * (D/2)]} \right) * \left( \frac{\delta\alpha}{\delta[\dot{x} * (D/2)]} \right) + A_r * \exp\left(-\frac{E_a}{R_g} * T\right) * \alpha^m * (1 - \alpha)^n \quad (71)$$

$$\frac{d\alpha}{d\tau} = \left( \frac{d}{d\dot{x}} \right) \left( \frac{d\alpha}{d\dot{x}} \right) + A * \exp\left(-\left(\frac{B}{\theta}\right) * (\alpha)^n * (1 - \alpha)^m\right) \quad (72)$$

This study investigates a large, pultruded panel of varying thickness using polyester resin and glass fibre reinforcement. A suitable mathematical model was used to predict whether the resin is fully and uniformly cured and whether there are any excess temperatures in the die. Equally, the model predicts the effect of controlling parameters like line speed, heater placement, configuration of Material on the conversion and temperature distribution. The conversion ( $\alpha$ ), and the temperature (T), distributions are governed by the following equations,

$$U_x \left( \frac{\delta\alpha}{\delta x} \right) = De \left[ \frac{\delta}{\delta z} \right] * \left[ \frac{\delta\alpha}{\delta z} \right] + \gamma \quad (73)$$

$$(\rho_c Cp_c) U_x \left[ \frac{\delta T}{\delta x} \right] = \lambda \left[ \frac{\delta T}{\delta z} \right] * \left[ \frac{\delta T}{\delta z} \right] - \rho_r \Delta Hr * \gamma \quad (74)$$

where  $U_x$  is the pulling speed;  $\rho_c Cp_c$  and  $\lambda$  the thermal properties of the composite, namely heat capacity and thermal conductivity;  $Hr$  the heat of reaction and  $\gamma$  the curing kinetics; and  $x$  the direction in which the part is being pultruded and  $y$  the distance from the centre of the part. The predictions of the curing process can be made using curing kinetics obtained from DSC and rheological experiments and combining them with thermal properties of glass fibre and polyester resin.

### 3.6. Influence on Heat flow during Pulling Operation.

The mathematical ‘partial differential equation (Eqs.67-74)’ based model, with dimensionless variables was used to predict the influence of die thickness on heat flow in terms of temperature. 3-D plot as shown in Figure (9a), precisely indicates dimensionless radial change has negligible effect on temperature but has profound after certain dimensionless time. After certain time, increment is observed with increasing radial distance but gets diminished beyond certain radial thickness. At small radial thickness, a small shoulder in temperature observed which insidiously increased at higher radial thickness and reaches peak value with increasing time.

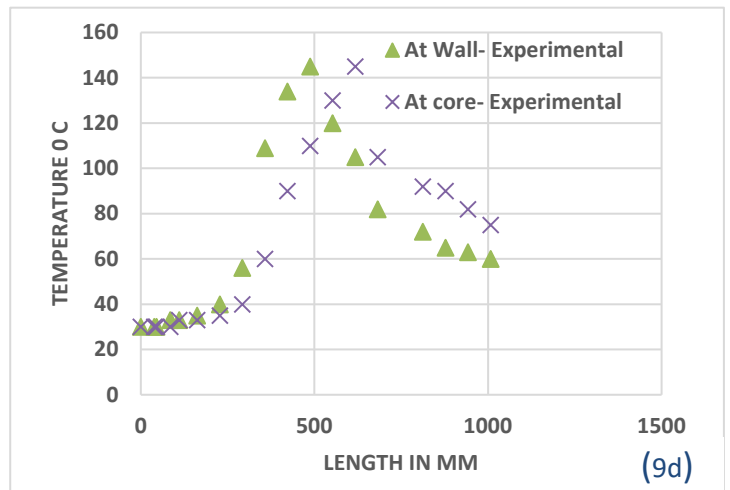
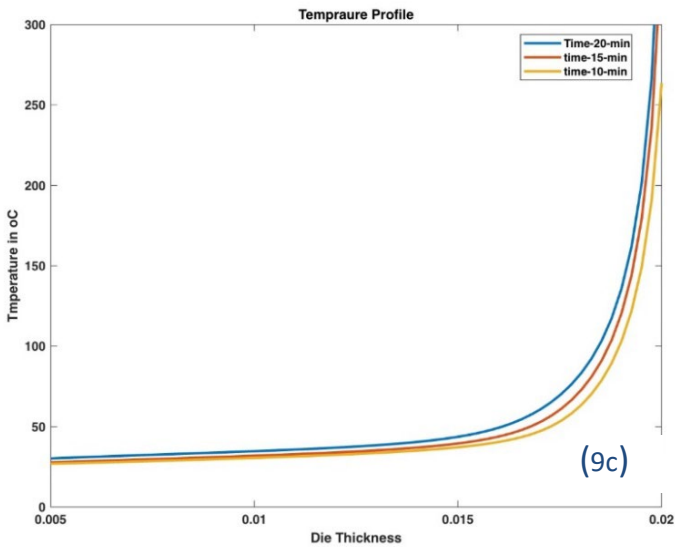
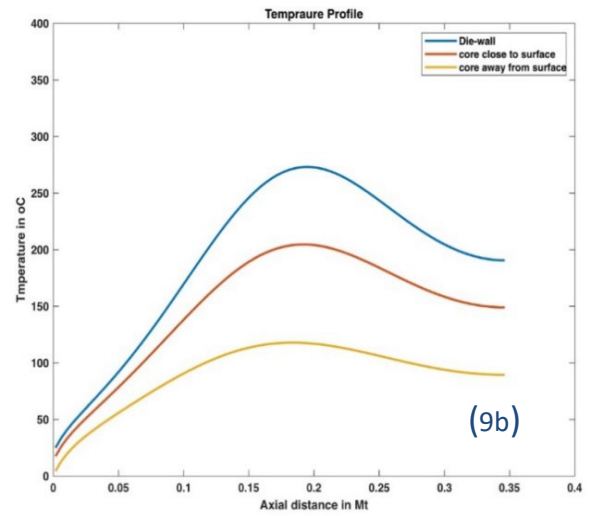
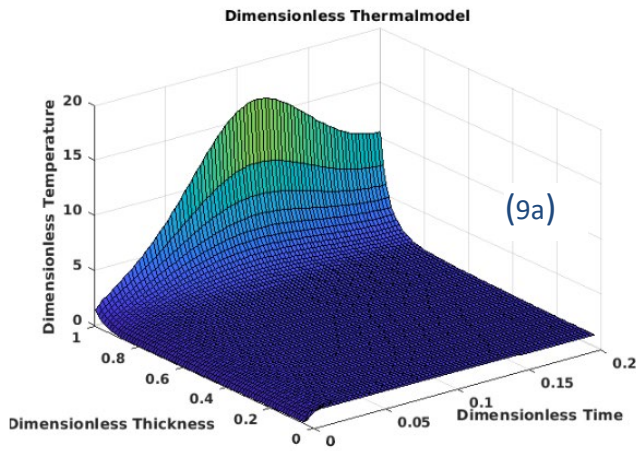


Figure (9a): Model fitting 3-D plot of dimensionless temperature against dimensionless time and thickness of die, (9b) : Model fitting -temperature profile along axial length for material close and away from die wall (9c) : Model fitting-temperature profile along radial thickness for material at different duration (9d) : Temperature profile as observed experimentally for material close and away from die wall.

As observed from dimensionless radial thickness, apparently implicates material in pultrusion die close to surface and away from core trajectory proclaims more profound and fast to its maximum value. Paradigm would be prominent and precise when real time temperature is plotted against axial distance as shown in Figure (9b). Temperature soars faster to its maximum value and trajectory maintain higher values with increased area under curve for materials at the die-wall compared to core, wherein materials away from surface/die wall always have lower

values with less area under curve implicates significant delay of heat transfer due to higher radial thickness, which show good agreement with experiment results as shown on Figure (9d). Equally, from Figure (9c), the paradigm as observed for certain holding time, temperature goes increasing with increasing radial thickness and found marginal difference in holding time. Hence, for early heating, on placing the band-heaters close to die entry, change in trajectory of soaring temperature is barely perceptible. Due to experimental difficulties to verify the temperature change with radial thickness, experiments were conducted along axial distance at early heating (heaters placed close to die entry) and for late heating (heaters placed away from die entry). Experimental results as shown in Figure (10a), are in good agreement with paradigm as observed from model, Figure (10b). Due to late heating, heat transfer to material close to core is low and that is being exhibited by less area under curve with low temperature profile throughout. Model was used to predict the influence of line speed on temperature and conversion of uncured part in the die along the axial pulling distance. Experimentally two different pultrusion line speeds of 168mm /min and 240 mm/min was maintained and found as shown in Figure (10d), reaction temperature spikes faster at lower line speed and lag-behind as speed increases along axial distance. Model confirms similar paradigm as shown in Figures (10c), on increasing pulling speed, residence time of the part inside die gets shortened, turn out low degree of conversion at same axial length compared to low speed. Stiff slop as observed for low speed clearly indicates early faster retransfer along axial length of the die. It is clear, that higher speed gets less chance to dissipate heat and showing low diminishing trend in temperature after peak. But larger area under curve at higher speed, is unable to legitimate with possible explanation. The curing of core takes longer time to flow heat through the thickness of the part and is just fully cured as it leaves the die exit. To promote faster curing heating profile at the die wall may be improved by extending the heating zone further down the die. However, such step should be taken cautiously as it may create uneven curing due to diffusion phenomena and the feasible solution would be to lengthen the die which in turn may significantly rise the pull force required.

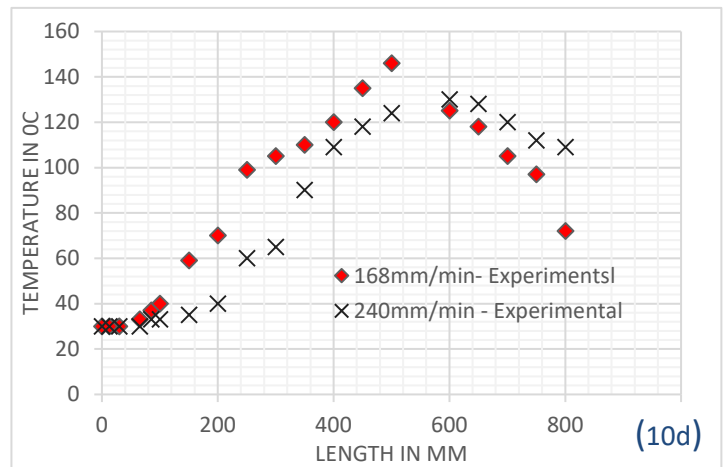
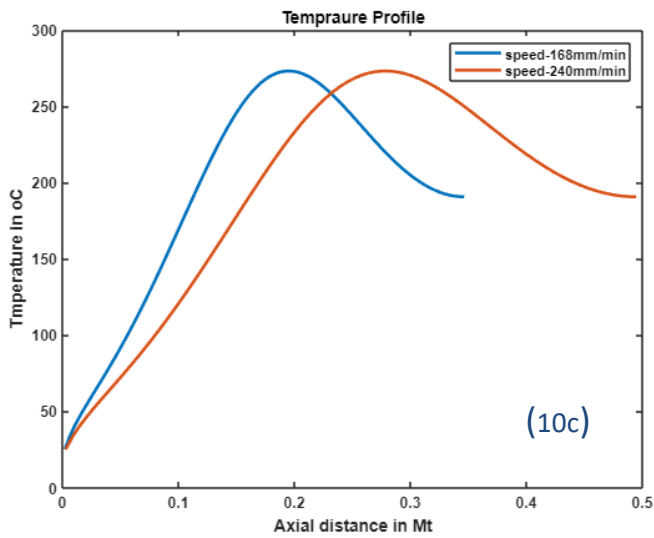
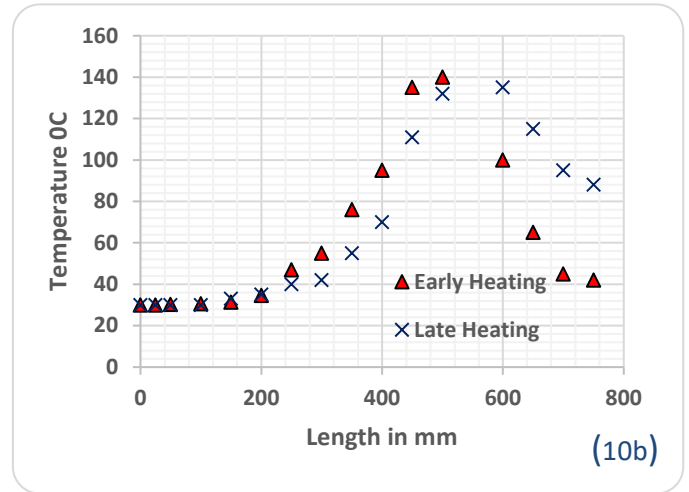
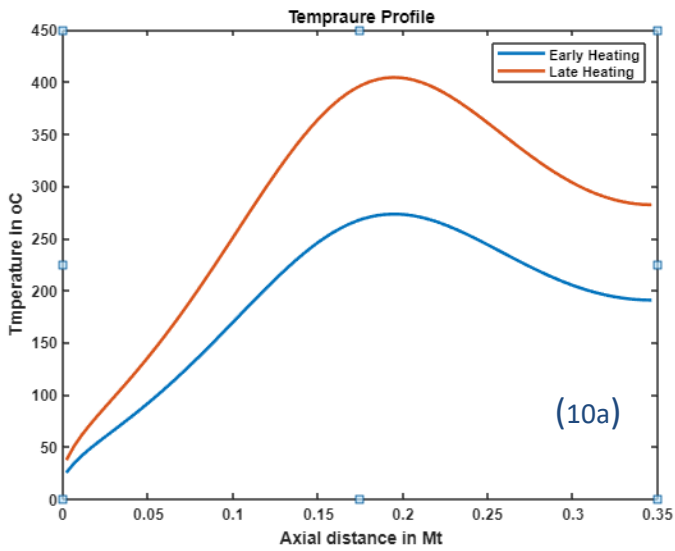


Figure (10a): Model fitting -Composite's Temperature profile along axial length for early and late heating by (10b): Model fitting -Composites' Temperature profile as observed experimentally along axial length for early and late heating (10c): Model fitting - Composite's temperature profile along axial length at 168mm/min and 240mm/min pulling speed (10d): Model fitting -Along axial length at 168mm/min and 240mm/min pulling speed

### 3.7. Influence on degree of conversion during Pulling Operation.

Using the developed mathematical ‘partial differential equation’ based model, the prediction on the trajectory of conversion and temperature along change in axial distance, speed and die thickness was made. Variables are converted to Dimensionless parameters in minimising

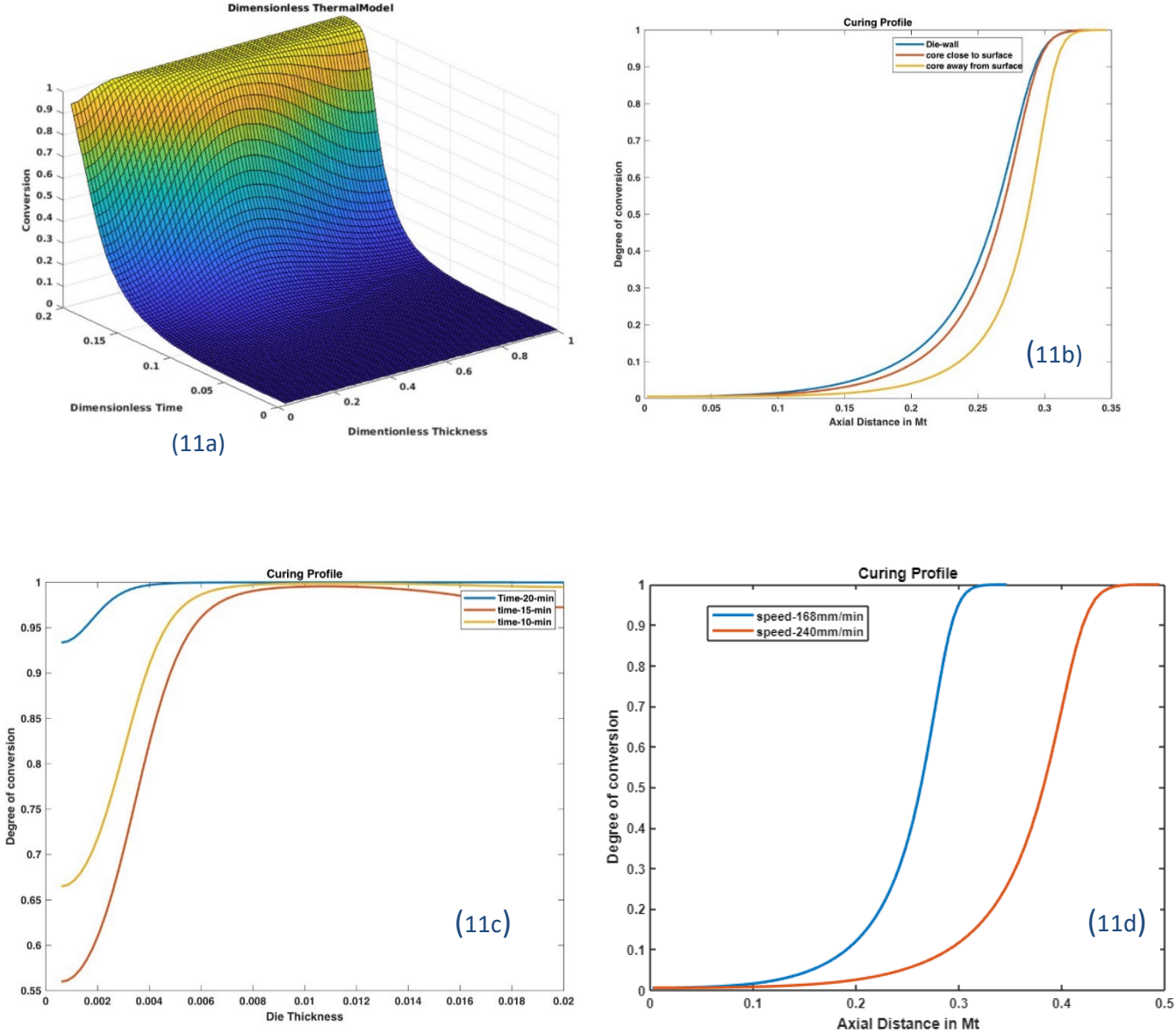


Figure (11a): Model fitting 3-D plot -Composite’s Degree of conversion with dimensionless time and thickness of die (11b): Model fitting -Composite’s Degree of conversion profile along axial Die length for material close and away from die wall (11c): Model fitting -Composite’s Degree of conversion profile along radial Die thickness for materials at different duration (11d): Model fitting - Composite’s Degree of conversion profile at 168mm/min and 240mm/min pulling speed

complexity of model. As found, in Figure (11a) a 3-D plot of conversion, dimensionless time and die thickness, degree of conversion increases insidiously and reaches peak value with increasing wherein material reaches to surface and away from core as apparently observed from dimensionless radial thickness, trajectory proclaims more profound and fast to its maximum value. Paradigm is clear and precise when real time degree of conversion is plotted against axial distance as shown in Figure (11b). Curing takes faster for materials at die wall compare to core but slope which implicates, completion is faster curing commence for early at die-wall where in completion does not have any significant delay. Perhaps delay in completion of curing observed for thick profiles. Early heating or higher rate of heating brings higher crosslinking or higher conversion at the beginning and release higher exothermic heat. Similarly, from Figure (11c), paradigm as observed for certain holding time, degree of conversion reaches to its maximum towards die-wall, but higher degree of conversion is found for higher holding time. Hence, for early heating, is achieved for placing the band-heaters close to die entry, spikes the curing process rather than late heating.

On the other hand, the model was used to predict the influence of line speed on temperature and conversion of uncured part in the die along the axial pulling distance of two different pultrusion line speeds of 168mm /min and 240 mm/min was maintained and found as the line speed increases, reaction conversion occurs and gets completed later along axial distance. Figure (11d) shows the influence of line speed on degree of conversion in the die along axial distance at certain radial thickness and die temperature. Residence time of the part inside die gets shortened on increasing pulling speed, turn out low degree of conversion at same axial length compared to low speed. Stiff slop as observed for low speed clearly indicates early conversion along axial length of the die. Hence increased pulling lowers rate of curing wherein part close to die wall cures faster compare to part in the core. So for thick part, lengthening Die is recommended but they may enhances pressure of pulling.

Eventhood attempt was made to comprehend the influences of puling speed, die thickness but it's difficult to capture other complex parameters to comprehended curing mechanism inside Die which solely controls the part properties.

#### **4. Conclusions**

In large scale pultrusion operation, effect of time and temperature on network formation plays crucial role. Present studies focused on predicting temperature distributions and conversion behaviour in die during pultrusion operation. The study even elucidates the effect of line speed,

heating rate and part thickness on curing process. In this work, kinetic and rheological data have been modelled using measured by dynamic and isothermal DSC and viscosity build-up. The governing equation shows good agreement with experimental data in predicting that the heater position relative to die entry has direct controls on rate of heating. Similarly, it is shown that the pulling speed influences heat flow and its convection. Again, prediction of heat transfer from die wall to core (i.e., thickness of the part being pulled) corresponds to the depth of the part and has major impact on part curing which eventually effects properties of the part.

## **Declarations**

### **Funding**

The authors are thankful to financial support for AM from Shapoorji Pallonji Group through secondment to Robert Gordon University for a Research Fellowship in a project titled 'Honeycomb Composite Structures for Ballistic Protection' Project No. 120437.

### **Conflicts of interest**

The authors have no conflicts of interest to declare that are relevant to the content of this article.

### **Availability of data and material**

The image data used will be provided on request.

### **Code availability (software application or custom code)**

The code used will be provided on request.

### **Ethics approval**

The authors declare no competing interests.

### **Consent to participate (include appropriate statements)**

N/A.

### **Consent for publication (include appropriate statements)**

N/A

### **Authors' contributions**

**AM:** Conceptualization, Investigation, Methodology, Writing - Original Draft, Writing - Review & Editing, Validation, Funding Acquisition. **NP:** Conceptualization, Methodology, Writing - Review & Editing, Resources, Funding Acquisition, Supervision. **JN:** Conceptualization, Methodology, Writing - Review & Editing, Project administration, Resources, Funding Acquisition, Supervision.

## References

- [1] Gadam S. U. K, Roux J. A, McCarty T. A, and Vaughan J. G, *Composites Science and Technology* 2000, vol. 60, no. 6, pp. 945–958,
- [2] N.S Shakya, J.A Roux, and A.L Jeswani, *Polymer Composites*. 2000 Oct;21(5):762-78.
- [3] W.B Young, *Polymer Composites* 1994, 15(2), pp1 18-127
- [4] Lin R, Lee L.J, and Liou M.J, *International Polymer Processing* 1991, 6(4), pp356-369,
- [5] Brennan M, Connolly M, Shidaker T.A, *Proceedings of the 9th World Pultrusion Conference*, European Pultruders Technical Association, March 2008.
- [6] Carlone P, Palazzo G. S, and Pasquino R, *Mathematical and Computer Modelling*, vol. 44, no. 7-8, pp. 701–709, 2006.
- [7] A Mukherji and J Njuguna, *4th International Conference on Structural Nano Composites (NANOSTRUC2018)*, Berlin, Germany, May 2018.
- [8] Y Bai., N. L Post, J. J Lesko, and T Keller *Thermochimica Acta*, 469: 28-35. (2008).
- [9] F Altaf, M B K Niazi, Z Jahan, T Ahmad, M A Akram, A safdar, M S Butt, T Noor , F Sher , *Journal of Polymers and the Environment* 2021; 29(1):156-174.
- [10] J Zhu, K Chandrashekhara, V Flanigan and S Kapila, *J Applied Polym Sci* 2004., Vol. 916, pp. 3513-3518.
- [11] Barkanov E, Akishin P, Namsone E., Bondarchuk A., and Pantelelis N, *Mechanics of Composite Materials, Vol. 56, No. 2, May, 2020*
- [12] Badrinarayanan P, Y. Lu, Larock R. C. and Kessler M. R., *Journal of Applied Polymer Science* 2009, 113: 1042-1049. Print.
- [13] Liang, G, and Chand Analytical Chemistry rashekhara K. *Journal of Applied Polymer Science* 2006. 102: 3168-3180. Print.
- [14] Boxel R V, Brennan M and Connolly M, *Huntsman Polyurethanes 2007, Everslaan 4 5, 3078 Everberg, Belgium.*
- [15] Kosar V, Gomzi Z 1, *European Polymer Journal* 2004, 40: 2793–2802
- [16] Kommu S, Khomara B. I and Kardos J. L, *Polymer Composites* 1998, 19(4), pp335-346,.
- [17] Huang H. C and Usmani A. S, *Finite element analysis for heat transfer*. Springer-Verlag, London, 1994.
- [18] Kosar V and Gomzi Z, *Chem. Biochem. Eng.* 2001, 15 (3) 101–108
- [19] Lin L. X, Crouch I. G, and Lam Y. C, *Composites Science and Technology* 2000, vol. 60, no. 6, pp. 857–864,.

- [20] Rita de C C D, Lizandro de S S, Ouziac H\_e, Schledjewskia R, *Materials Today Communications* 2018, 17; 362–370
- [21] L Sun, *PhD Theses*, Chemical engineering, Louisiana State University, 2002.
- [22] J. M Barton, I Hamerton, B. J Howlin, J. R Jones, and S Liu, *Polymer* (1998),
- [23] Boey F. Y. C. and W Qiang, *Journal of Applied Polymer Science* (2000), 78, 511  
39, 1929
- [24] Min Hu, Demei Yu, Jianbo Wei, *Polymer Testing* 2007, 26 ;333–337.
- [25] Z Jahan, M B K Niazi, S Gul, F Sher, S J Kakar, M-B Hägg, Y W Gregersen, *Journal of Polymers and the Environment*, 2021;29: 2598-2608.
- [26] Lam P. W. K, *Polymer Composites* 1987, vol. 8, pp. 427-436
- [27] N Sbirrazzuoli,, S Vyazovkin, A Mititelu, C Sladic, and L Vincent.. *Macromolecular Chemistry and Physic* (2003): s. 204.15 1815-1821. Print.
- [28] J Michaud., A BERIS. N, and P. S Dhurjati., *Journal of composite materials* 2002, vol. 36, pp. 1175-1200,
- [29] A Mukherji, S Patil, *6<sup>th</sup> Recent Advancement on Polymer Technology, National conformance*, India, Jan,2017,
- [30] Dupuy J, Leroy E, and Maazouz, A, *Journal of Applied Polymer Science* 2000, 78, 2262.
- [31] Price D.M, Jarratt M, *Thermochim. Acta* 2002,392–393 ;231[30]
- [32] Mukherji A, Tarapure ND, Wakure GN, *3rd International Conference on Structural Nano Composites (NANOSTRUC2016) IOP Publishing IOP Conf. Series: Materials Science and Engineering* 2017, 195
- [33] Yu Bai, T Valle'e, T Keller, *Composites Science and Technology* 67 (2007) 3098–3109.
- [34] A Mukherji, 4th Annual National conference India, Jan, 2017,

## **Caption of Figures and Tables**

Table 1. Materials and formulation used for the friction measurement

Figure 1(a): Schematic diagram of open bath pultrusion studied Figure  
1(b): The schematic of Compaction Zone in Conventional Pultrusion Die with 100 mm  
discontinuity gap

Figure2: Dynamic DSC of formulated polyester resin.

Figure 3: TGA profiles. (a) TGA profiles for the formulated Polyester resin at different temperature, (b) TGA thermograms of red is recycled polymer fibres/felt, black is polyester (composite) prepreg with recycled polymers fibres as reinforced, green is pure polyester resin

Figure 4: Change in viscosity of formulated rein with time sweep at different set temperature

Figure (5a): Model fitting- Kissinger plot for activation energy of formulated resin.  
(5b): Rate of heat evolution during cure reaction

Figure (6a): Model fitting-degree of conversion with temperature sweep  
(6b): Change in rate of conversion with degree of conversion at DSC mood

Figure 7: Model fitting -rate of conversion of monomers with time sweep at three different set temperature

Figure (8a): Thermal resistance with volume-area ratio for resin  
(8b): Thermal resistance with volume-area ratio for recycled felts, used as reinforcing materials.

Figure (9a): Model fitting 3-D plot of dimensionless temperature against dimensionless time and thickness of die, (9b) : Model fitting -temperature profile along axial length for material close and away from die wall (9c) : Model fitting-temperature profile along radial thickness for material at different duration (9d) : Temperature profile as observed experimentally for material close and away from die wall.

Figure (10a): Model fitting -Composite's Temperature profile along axial length for early and late heating by (10b): Model fitting -Composites' Temperature profile as observed experimentally along axial length for early and late heating (10c): Model fitting - Composite's temperature profile along axial length at 168mm/min and 240mm/min pulling speed (10d): Model fitting -Along axial length at 168mm/min and 240mm/min pulling speed

Figure (11a): Model fitting3-D plot -Composite's Degree of conversion with dimensionless time and thickness of die (11b): Model fitting -Composite's Degree of conversion profile along axial Die length for material close and away from die wall (11c): Model fitting -Composite's Degree of conversion profile along radial Die thickness for

materials at different duration (11d): Model fitting - Composite's Degree of conversion profile at 168mm/min and 240mm/min pulling speed

### Nomenclature & Symbols

Symbols	Nomenclature	Symbols	Nomenclature
$\rho / \rho_r / \rho^c$	Density of tool/resin/composites	$V_r$	Resin Volume Fraction
$C_p / C_{p_r} / C_{p_c}$	Specific heat of tool/resin/composites	$H_r$	Total Heat Generation by resin During Curing at Specific Temperature.
$K_{x/y/z}$	Thermal conductivity of composite in x/y/z direction	$B$	Heating Rate
$K_c$	Thermal conductivity of tool	$T_p$	Peak Temperature
$\lambda_{1/2/3}$	Thermal conductivity of prepreg of low volatile, resin and Reinforcements	$A$	pre-exponential factor
$V$	Seepage velocity	$T^*$	Temperature at which $k=1$
$V_{1/2/3}$	Volume of the respective low volatile, resin and Reinforcements	$T$	Temperature in Kelvin
$v$	Velocity of resin at Gel	$T_{1/2}$	Temperature at which $\dot{K}=1$
$R$	Thermal resistance	$T_0$	Initial Temperature
$Q$	Heat Transfer Rate	$\alpha$	Degree of Crosslinking
$L$	Length of the sample	$\eta_0$	Initial viscosity

$\eta$	Viscosity at Specific Temperature	$A_\eta$	initial viscosity at $T = \infty$
$H_t$	Total Heat of Reaction	$E_n$	<i>Activation Energy at Viscous flow</i>
$\varphi$	<i>Fibre Porosity</i>	$E_a$	<i>Activation Energy</i>
$\frac{\delta T}{\delta t}$	Rate of Heating	$\dot{x}$	Dimensionless Radius
$\frac{\delta T}{\delta x}$	Gradient of Heating in x-direction	$\tau$	Dimensionless time
$Ux$	Speed of Pulling	$\dot{K}$	Equilibrium Reaction Constant
$De$	molecular diffusivity of the composite.	$\theta$	Dimensionless Temperature
$\gamma = \left(\frac{\delta \alpha}{\delta t}\right)$	Rate of Conversion/curing Kinetic	$\dot{\alpha}$	Thermal Diffusivity
$m$	Autocatalytic cure reaction order	$n$	Autocatalytic cure reaction order
$\left(\frac{\delta \alpha}{\delta x}\right)$	Gradient of degree of Crosslinking	$R_g$	Gas Constant
$\left(\frac{\delta T}{\delta z}\right)$	Gradient of Temperature	$K$	Rate constant
$\frac{d\alpha}{d\tau}$	Change of Degree of Crosslinking with Dimensionless time	$A_r$	Arrhenius Number
$\Delta Hr$	Difference of Heat	$A$	Contact Area of the sample